

Master Stability Functions for metacommunities with two types of habitats

Alexander Krauß,^{1,*} Thilo Gross,^{2,3,4,†} and Barbara Drossel^{1,‡}

¹*Technical University of Darmstadt, Institute for Condensed Matter Physics, Hochschulstr. 6, 64289 Darmstadt*

²*Helmholtz Institute for Functional Marine Biodiversity,
University of Oldenburg (HIFMB), Ammerländer Heerstraße 231, 26129 Oldenburg.*

³*Alfred-Wegener-Institute for Marine and Polar Research,
Bremerhaven, Germany, Am Handelshafen 12, 27570 Bremerhaven.*

⁴*University of Oldenburg, Oldenburg, Germany, Ammerländer Heerstraße 114-118, 26129 Oldenburg.*

(Dated: September 3, 2021)

Current questions in ecology revolve around instabilities in the dynamics on spatial networks and particularly the effect of node heterogeneity. We extend the Master Stability Function formalism to inhomogeneous biregular networks having two types of spatial nodes. Notably, this class of systems also allows the investigation of certain types of dynamics on higher-order networks. Combined with the Generalized Modelling approach to study the linear stability of steady states, this is a powerful tool to numerically assess the stability of large ensembles of systems. We analyze the stability of ecological metacommunities with two distinct types of habitats analytically and numerically in order to identify several sets of conditions under which the dynamics can become stabilized by dispersal. Our analytical approach allows general insights into stabilizing and destabilizing effects in metapopulations. Specifically, we show that maladaptive dispersal may be stable under certain conditions.

I. INTRODUCTION

Understanding the factors that stabilize or destabilize nonlinear dynamics on complex networks is important for conservation, design, or control, depending on the type of system. Examples are ecological networks, regulatory networks in biological cells, electrical power networks, or human traffic networks. Many of these systems can be conceptualized as complex multi-layer and/or higher order networks. This allows for a richer more detailed description of the system but complicates the analysis of the dynamics.

For instance, in ecology plant-pollinator networks are coupled to herbivores that feed on the plants, and this can reduce the nestedness of the plant-pollinator network [1]. The spatial coupling of chemical reaction networks in different biological cells or of local foodwebs on different habitat patches can give rise to Turing and wave instabilities that destroy steady states that would be stable in a spatially isolated network [2, 3].

Further spatial coupling of a heterogeneous set of networks can stabilize networks that would be unstable otherwise, for instance in ecological source-sink systems [4–8]. The theoretical study of these multilayer systems is hampered by the computational costs that increase rapidly with the number of nodes and the number of parameters and possible network structures to be explored.

An elegant tool to deal with the vast parameter space and the great variety of possible models is Generalized Modeling (GM) [9], which focuses on linear stability of steady states and expresses the Jacobian of the system

in terms of scale parameters and exponent parameters. Scale parameters quantify the relative contributions of the different types of gain and loss terms to the overall turnover of each species. Exponent parameters quantify how the different growth and loss terms change with the population sizes in the vicinity of the considered steady state. By specifying the ranges of these parameters, a general class of models can be investigated without the need to precisely fix the functional forms of the growth and loss terms.

In networks with homogeneous nodes stability analysis can build on master-stability functions (MSF). This idea is commonly credited to [10] who used it to study oscillator synchronization. However, the mathematical formalism was already used in ecology by Othmer and Scriven [11] in the context of pattern formation and was subsequently applied to complex networks by Segel and Levin [12] and is also discussed in [13, 14].

The combination of generalized models and master stability functions was already used in [3] to study a multiplex meta-foodweb [15]. These models describes a geographical network of M habitat patches. Each of these patches is home to a complex food web of N species, such that the dynamical dimension of the model is NM and stability of steady states is captured by a Jacobian matrix of size $MN \times NM$. The GM+MSF approach disentangles the influence of the structure of the spatial network on stability from that of the local species network such that stability can be decided by examining the eigenvalues of an $N \times N$ and an $M \times M$ matrix. Besides computational efficiency, the approach thus provides a deeper understanding of how the spatial and the ecological network structures impact stability.

This MSF approach builds on the assumption that all nodes of the spatial network are equivalent, so that the species network has the same steady state on all habi-

* alexander.krauss@pkm.tu-darmstadt.de

† thilo.gross@hifmb.de

‡ drossel@pkm.tu-darmstadt.de

tats. Recently, this approach was extended to the case where only part of the species have populations on all habitats, while others are global species that have a single population that couples to its interaction partners on all habitats simultaneously [16].

In this paper, we develop a generalization of the Master-Stability-Function approach to biregular heterogeneous systems, namely to meta-networks with different types of spatial nodes. These systems are regular graphs in the sense that every node of a given type is connected to the same number of neighboring nodes. Moreover, they are bipartite such that a node of a given type only interacts with the nodes of the respectively other type.

Our motivation for choosing this particular system is twofold. First, from a purely operational perspective it provides a framework in which analytical insights can be gained which allows a deeper understanding of the important ecological question of node heterogeneity. Second, we are motivated by recent work on dynamics on hypergraph/higher order dynamical networks [17, 18], which under certain conditions map to the biregular system class.

In the ecological context the biregular system provides an adequate model for the dispersal of individuals between patches. When dispersing many higher animals enter a roaming state where they are in transit between patches while looking for a new home range. In this roaming state population dynamics (typically dominated by losses) can still occur such that there is population dynamics both on the links and the nodes of the geographical network, similar to the model in [17]. Representing the nodes in a regular graph by one node type and the links connecting them as another node type leads to a biregular network of the type considered here.

These ecological systems belong to the wider class of source-sink systems, which are ubiquitous in heterogeneous landscapes. Sources are high quality habitats where populations exhibit a positive net growth rate, while sinks are poor quality habitats with negative net growth rates. Coupling the two types of habitats can maintain populations in sinks that would otherwise go extinct, and outflow from sources as well as inflow from sinks can affect the stability of sources.

Dispersal between sources and sinks cannot only happen through passive dispersal, but also through adaptive dispersal, for instance from overcrowded sources to lower quality but less crowded habitats [5, 19]. Such active dispersal can, however, also be maladaptive [20, 21]. A particular risk to wildlife are perceptual and ecological traps, where individuals disperse actively out of high-quality habitats or into low-quality habitats and thereby reduce their rate of reproduction [22]. Many of these traps are due to recent changes caused by human interference [23], such as reflecting artificial surfaces which attract mating water insects [24, 25], or developed mountain valleys that attract grizzly bears [26]. Albeit detrimental to the population size, traps might sometimes help to stabilize population dynamics [27]. As a specific application of the

methodological development presented in this paper, we will show that such stabilizing effects of perceptual and ecological traps are indeed possible under generic conditions.

In the following, we first develop the generalized Master-Stability-Function formalism for meta-networks with two types of spatial nodes. Then, we define a class of generalized ecological models of which the stability is explored with this method. We find that there are two types of dispersal turnover rates in source-sink dynamics, and specify general conditions under which increasing dispersal rates can have a stabilizing effect. Analytical calculations for one species in source-sink systems are supplemented by numerical evaluations of systems with foodwebs consisting of several species, giving similar stability conditions. Among these conditions, we will identify a subset that demonstrates a stabilizing effect of traps.

II. DIFFUSION-DRIVEN INSTABILITIES FOR TWO TYPES OF PATCHES

We consider a system of N species and M patches. The dynamics for the population size X_i^k of species i on patch k of a meta-network such as an ecological meta-community has the general form

$$\dot{X}_i^k = G_i^k(\mathbf{X}^k) - M_i^k(\mathbf{X}^k) + \sum_{l=1}^M E_i^{kl}(\mathbf{X}^k, \mathbf{X}^l) - \sum_{l=1}^M E_i^{lk}(\mathbf{X}^l, \mathbf{X}^k). \quad (1)$$

The first term describes local growth in patch k due to primary production (for plants) and consumption of other species, the second local losses (“mortality”) due to predation and other causes of death, and the last two terms describe dispersal into and out of patch k . We assume that there are two types of patches, which we will call sources and sinks, with sources having a positive net growth rate $G_i^k(\mathbf{X}^k) - M_i^k(\mathbf{X}^k)$ and sinks having a negative one. We further assume that all sources have identical parameters (including patch size) and all sinks have identical parameters. The numbers of sources (M^+) and of sinks (M^-) will in general be different. We furthermore assume that sources are connected only to sinks and vice versa. In order to obtain identical steady states for all patches of the same type, they must have the same degree, thus the network has to be biregular. This means that at a steady state the population sizes of all source patches are identical, $(\mathbf{X}^k)^* = \mathbf{X}^+$ for $k \in \{1, \dots, M^+\}$ and those of all sinks are identical, $(\mathbf{X}^k)^* = \mathbf{X}^-$ for $k \in \{M^+ + 1, \dots, M^+ + M^-\}$.

The stability of a steady state is determined by the Jacobian

$$\mathbf{J}_{(i+kN)(j+mN)} = \left. \frac{\partial \dot{X}_i^k(\mathbf{X})}{\partial X_j^m} \right|_{\mathbf{X}=\mathbf{X}^*}. \quad (2)$$

When we separate the within-patch and between-patch terms, \mathbf{J} has entries of the form

$$\begin{aligned}\frac{\partial \dot{X}_i^k}{\partial X_j^k} &= \mathbf{P}_{ij}^k - \sum_{l=1}^M \mathbf{C}_{ij}^{kl} \\ \frac{\partial \dot{X}_i^k}{\partial X_j^l} &= \hat{\mathbf{C}}_{ij}^{kl}\end{aligned}\quad (3)$$

with the matrix elements that result from taking the derivatives of G and M in (1) being included in \mathbf{P} , and those that involve the dispersal terms E entering the matrices \mathbf{C} and $\hat{\mathbf{C}}$. Since the three types of matrices are identical for all patches of the same type, we can express the Jacobian in the compact block form

$$\mathbf{J} = \begin{pmatrix} \mathbf{I}^+ \otimes (\mathbf{P}^+ - d^+ \mathbf{C}^+) & \mathbf{M} \otimes \hat{\mathbf{C}}^+ \\ \mathbf{M}^T \otimes \hat{\mathbf{C}}^- & \mathbf{I}^- \otimes (\mathbf{P}^- - d^- \mathbf{C}^-) \end{pmatrix}, \quad (4)$$

where \mathbf{I}^+ (\mathbf{I}^-) is the identity matrix of dimension M^+ (M^-), and the matrix \mathbf{M} denotes which patches are connected. It has M^+ rows and M^- columns. We allow multiple links between the same pair of patches. Since all patches of one type have the same degree, \mathbf{M} has a constant row sum equal to the source's degree d^+ and a constant column sum equal to the sink's degree d^- . The symbol \otimes denotes the Kronecker product.

The eigenvalues λ of the Jacobian are obtained by solving

$$\mathbf{J}\mathbf{u} = \lambda\mathbf{u}. \quad (5)$$

The specific form (4) enables us to reduce the degree of this equation similarly to what has been done with the Master-Stability Function (MSF) approach by Brechtel et al. [3]. To this purpose, we make the ansatz

$$\mathbf{u} = \begin{pmatrix} \mathbf{w}^+ \otimes \mathbf{v}^+ \\ \mathbf{w}^- \otimes \mathbf{v}^- \end{pmatrix}. \quad (6)$$

The N -dimensional normalized vectors \mathbf{v}^+ and \mathbf{v}^- give the contribution of the different species to the eigenvectors within sources and sinks, and \mathbf{w}^+ and \mathbf{w}^- denote the weights of these eigenvectors on the different source and sink patches.

In the following, we will show that we can find all solutions of the eigenvalue equation (4) by specifying that

$$\mathbf{M}^T \mathbf{w}^+ = \beta \mathbf{w}^- \quad \text{and} \quad \mathbf{M} \mathbf{w}^- = \alpha \mathbf{w}^+. \quad (7)$$

Inserting this together with the ansatz (6) into the eigenvalue equation (5) leads to a reduced eigenvalue equation with a reduced Jacobian \mathbf{j} ,

$$\begin{aligned}\mathbf{j} \begin{pmatrix} \mathbf{v}^+ \\ \mathbf{v}^- \end{pmatrix} &\equiv \begin{pmatrix} \mathbf{P}^+ - d^+ \mathbf{C}^+ & \alpha \hat{\mathbf{C}}^+ \\ \beta \hat{\mathbf{C}}^- & \mathbf{P}^- - d^- \mathbf{C}^- \end{pmatrix} \begin{pmatrix} \mathbf{v}^+ \\ \mathbf{v}^- \end{pmatrix} \\ &= \lambda \begin{pmatrix} \mathbf{v}^+ \\ \mathbf{v}^- \end{pmatrix},\end{aligned}\quad (8)$$

provided that \mathbf{w}^+ and \mathbf{w}^- are nonvanishing. This reduced Jacobian is of dimension $2N$ instead of MN . The

influence of topology is captured in the coefficients α and β . One class of solutions for \mathbf{w}^- and \mathbf{w}^+ can be obtained by transforming (7) to

$$\alpha\beta\mathbf{w}^+ = \mathbf{M}\mathbf{M}^T\mathbf{w}^+ \quad (9)$$

or

$$\alpha\beta\mathbf{w}^- = \mathbf{M}^T\mathbf{M}\mathbf{w}^-. \quad (10)$$

Thus the positive roots $\sqrt{\alpha\beta}$ are the singular values[28] of \mathbf{M} , i.e., $\alpha\beta$ are the joint eigenvalues of $\mathbf{M}\mathbf{M}^T$ and $\mathbf{M}^T\mathbf{M}$. Their quantity is $\min\{M^+, M^-\}$. The largest of these singular values is $\sqrt{d^+d^-}$ because $\mathbf{M}^T\mathbf{M}$ and $\mathbf{M}\mathbf{M}^T$ have a constant row sum of d^+d^- . The reduced eigenvalue equation (8) for λ depends only on the product $\alpha\beta$, thus we can choose

$$\alpha = \beta \quad (11)$$

without loss of generality. Since $\mathbf{M}^T\mathbf{M}$ and $\mathbf{M}\mathbf{M}^T$ are symmetric and positive semidefinite, all of their eigenvalues are real and non-negative, i.e. $0 \leq \beta^2 \leq d^+d^-$. From this, we find $2N * \min\{M^+, M^-\}$ eigenvalues of the full Jacobian \mathbf{J} in equation (4) by solving the reduced eigenvalue equation (8) for each singular value $\beta \in S$, with S being the set containing all singular values of \mathbf{M} .

The remaining solutions are related to eigenvalues $\alpha\beta = 0$ of $\mathbf{M}\mathbf{M}^T$ or $\mathbf{M}^T\mathbf{M}$, whichever of these two matrices has the larger dimension. This matrix has $|M^+ - M^-|$ eigenvalues 0 in addition to the singular values of \mathbf{M} (among which there might also be 0s). We find the solutions associated with this eigenvalue by setting $\alpha = 0$ and $\mathbf{w}^- = 0$ in (7) if $M^+ > M^-$, and $\beta = 0$ and $\mathbf{w}^+ = 0$ otherwise. The eigenvalue equation (5) simplifies in this case to the two equations

$$\mathbf{M}^k \mathbf{w}^k = 0 \quad (12a)$$

$$(\mathbf{P}^k - d^k \mathbf{C}^k) \mathbf{v}^k = \lambda \mathbf{v}^k \quad (12b)$$

where $k = +$ and $\mathbf{M}^+ = \mathbf{M}^T$ if $M^+ > M^-$ and $k = -$ and $\mathbf{M}^- = \mathbf{M}$ if $M^- > M^+$. The corresponding modes are nonvanishing only on the more numerous type of patches. This gives $N|M^+ - M^-|$ additional solutions of equation (5). Altogether we thus have found all $2N * \min\{M^+, M^-\} + N * |M^+ - M^-| = NM$ solutions of the full eigenvalue equation for \mathbf{J} . Compared to the direct calculation of the eigenvalues of \mathbf{J} , this procedure saves a significant amount of computation time when the system has many patches.

The largest singular value $\beta = \sqrt{d^+d^-}$ is obtained when \mathbf{w}^+ and \mathbf{w}^- are vectors with all entries being 1. In this case, the dynamics close to the steady state are equivalent for all source and sinks patches respectively, and the associated eigenvalues are those of a system with one source and one sink patch. Since all eigenvalues λ must be negative for a stable steady state, the steady state of the M -patch system can only be stable if the corresponding two-patch system is stable.

However, stability of the two-patch system is not sufficient for stability of the entire network, as inhomogeneous modes, which have different amplitudes on different source and/or sink patches, may also be unstable, leading to a generalized version of diffusion-driven Turing instabilities or of wave instabilities.

III. GENERALIZED MODELING OF SOURCE-SINK DYNAMICS

In order to evaluate the stability of source-sink meta-communities, we use the generalized modeling approach [9]. By normalizing all population sizes and functions to their values at the considered steady state, equation (1) takes the form

$$\begin{aligned} \dot{x}_i^k = & \alpha_i^k \left[\nu_i^k g_i^k(\mathbf{x}^k) - \rho_i^k m_i^k(\mathbf{x}^k) + \frac{1 - \nu_i^k}{d^k} \sum_{l=1}^M e_i^{kl}(\mathbf{x}^k, \mathbf{x}^l) \right. \\ & \left. - \frac{1 - \rho_i^k}{d^k} \sum_{l=1}^M e_i^{lk}(\mathbf{x}^l, \mathbf{x}^k) \right], \end{aligned} \quad (13)$$

with $x_i^k = X_i^k / (X_i^k)^*$ and $g_i^k(\mathbf{x}^k) = G_i^k(\mathbf{X}^k) / (G_i^k(\mathbf{X}^k))^*$ and similarly for the other three functions. The coefficients α_i^k sets the time scale and is the total per-capita biomass turnover of the population at the steady state. The scale parameter ν_i^k denotes the relative contribution of production to total growth, and therefore $1 - \nu_i^k$ is the relative contribution of immigration to total growth. Likewise ρ_i^k and $1 - \rho_i^k$ denote the relative contributions of mortality and emigration to the total loss.

The d^k denote the degree of patch k , and each of the sums has exactly d^k nonzero terms. In general, dispersal may be dependent on population density and even on other species, such as a predator or prey, on the patch of origin or destination. By considering dependencies on other populations in the dispersal terms, we will be able to model adaptive and maladaptive movement.

At the steady state, we have $\dot{x}_i^k = 0$, and all functions take the value 1. This means that the difference between growth and mortality is equal to the difference between immigration and emigration.

We will choose a form of equation (13) that naturally reflects the differences between sources and sinks. Local production is larger than local mortality in sources and vice versa in sinks. Similarly, the rate of emigration is larger than that of immigration for sources and smaller than that of immigration for sinks. By making appropriate parameter substitutions, taking into account that all sources have the same set of parameters, and all sinks have the same set of parameters, we can write equation

(13) as

$$\begin{aligned} \dot{x}_i^{k+} = & \alpha_{P_i}^+ \left[g_i^{k+}(\mathbf{x}^{k+}) - m_i^{k+}(\mathbf{x}^{k+}) \right] \\ & + \alpha_{S_i}^+ \left[g_i^{k+}(\mathbf{x}^{k+}) - \frac{1}{d^+} \sum_{k_-} e_i^{k_-k+}(\mathbf{x}^{k_-}, \mathbf{x}^{k+}) \right] \\ & + \alpha_{C_i}^+ \left[\frac{1}{d^+} \sum_{k_-} e_i^{k_+k_-}(\mathbf{x}^{k+}, \mathbf{x}^{k_-}) \right. \\ & \left. - \frac{1}{d^+} \sum_{k_-} e_i^{k_-k+}(\mathbf{x}^{k_-}, \mathbf{x}^{k+}) \right] \end{aligned} \quad (14)$$

for all sources and

$$\begin{aligned} \dot{x}_i^{k-} = & \alpha_{P_i}^- \left[g_i^{k-}(\mathbf{x}^{k-}) - m_i^{k-}(\mathbf{x}^{k-}) \right] \\ & + \alpha_{S_i}^- \left[\frac{1}{d^-} \sum_{k_+} e_i^{k_+k-}(\mathbf{x}^{k_+}, \mathbf{x}^{k-}) - m_i^{k-}(\mathbf{x}^{k-}) \right] \\ & + \alpha_{C_i}^- \left[\frac{1}{d^-} \sum_{k_+} e_i^{k_-k_+}(\mathbf{x}^{k_-}, \mathbf{x}^{k_+}) \right. \\ & \left. - \frac{1}{d^-} \sum_{k_+} e_i^{k_+k_-}(\mathbf{x}^{k_+}, \mathbf{x}^{k_-}) \right] \end{aligned} \quad (15)$$

for all sinks.

FIG. 1 illustrates the relationship between the old and new parameters. The new turnover rates have an intuitive meaning that will be useful for the stability analysis further below. $\alpha_{P_i}^k$ captures the turnover due to local dynamics. In sources $\alpha_{P_i}^+$ is equal to the mortality rate and in sinks $\alpha_{P_i}^-$ is equal to the growth rate. Turnover due to dispersal is denoted with $\alpha_{C_i}^k$, with $\alpha_{C_i}^+$ being the rate of immigration to sources and $\alpha_{C_i}^-$ the rate of emigration from sinks. We therefore call it dispersal turnover. In addition to these two rates, there is an excess growth (not compensated by mortality) and an excess emigration (not compensated by immigration) in sources, and an excess mortality and immigration in sinks. This excess leads to a net source-sink flow rate $\alpha_{S_i}^k$. It is a direct measure of the strength of source-sink dynamics, which are absent if $\alpha_{S_i}^k = 0$. We have thus two distinct types of dispersal rates in source-sink dynamics. The rate $\alpha_{C_i}^k$ is due to dispersal out of sinks and into sources, while $\alpha_{S_i}^k$ is the rate of net source-sink flow driven by excess growth in sources. Below, we will investigate the impact of these two scale parameters on stability.

In addition to the relationships between turnover rates mentioned so far, there is the additional condition that the total biomass outflow from patch l into patch k has to be identical to the biomass inflow into patch k from patch l , requiring that

$$\alpha_i^l (1 - \rho_i^l) \frac{X_i^{l*}}{d^l} = \alpha_i^k (1 - \nu_i^k) \frac{X_i^{k*}}{d^k}. \quad (16)$$

Applying condition (16) to the situation where l is the sink and k is the source, and to the opposite situation,

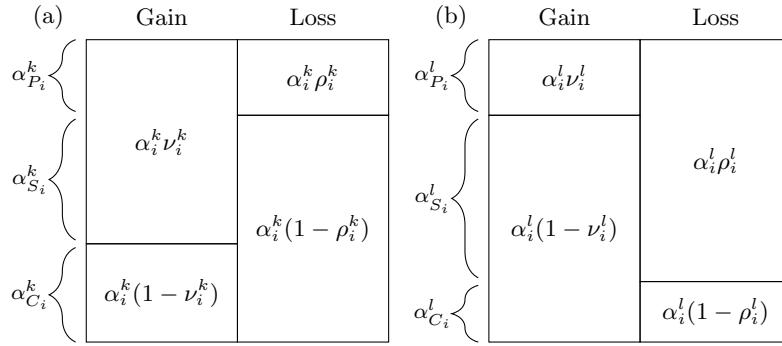


FIG. 1. Illustration of the relation between the original scale parameters in equations (13) and the turnover rates introduced in equations (14) and (15) for (a) sources and (b) sinks.

we obtain

$$q\alpha_{C_i}^+ = \alpha_{C_i}^- \quad \text{and} \quad q\alpha_{S_i}^+ = \alpha_{S_i}^- \quad (17)$$

with

$$q = \frac{X_i^{+*} d^-}{X_i^{-*} d^+}. \quad (18)$$

These consistency relations link the non-local turnover rates in sources and sinks through the tunable parameter q . Since the turnover rates and the parameter q can be varied independently, we can change turnover rates while keeping the population sizes constant.

We will base our stability analysis on the Jacobian of the normalized equations (13),

$$\mathbf{J}_{(i+kN)(j+mN)} = \left. \frac{\partial \dot{x}_i^k(\mathbf{x})}{\partial x_j^m} \right|_{\mathbf{x}=\mathbf{x}^*}. \quad (19)$$

It has the same eigenvalues as the Jacobian (2) and can be evaluated for our biregular system eqs. (14) and (15) with the methods described in section II.

For evaluating the Jacobian we need the derivatives of the normalized functions at the steady state, which are the so-called exponent parameters. In our model, we have the following exponent parameters:

$$\begin{aligned} \phi_i^k &= \left. \frac{\partial}{\partial x_i^k} g_i^k(x_i^k) \right|_{\mathbf{x}=\mathbf{x}^*}, & \mu_i^k &= \left. \frac{\partial}{\partial x_i^k} m_i^k(x_i^k) \right|_{\mathbf{x}=\mathbf{x}^*}, \\ \phi_{ij}^k &= \left. \frac{\partial}{\partial x_j^k} g_i^k(x_i^k) \right|_{\mathbf{x}=\mathbf{x}^*}, & \mu_{ij}^k &= \left. \frac{\partial}{\partial x_j^k} m_i^k(x_i^k) \right|_{\mathbf{x}=\mathbf{x}^*}, \\ \hat{\omega}_i^{kl} &= \left. \frac{\partial}{\partial x_i^k} e_i^{kl}(\mathbf{x}^k, \mathbf{x}^l) \right|_{\mathbf{x}=\mathbf{x}^*}, \\ \omega_i^{kl} &= \left. \frac{\partial}{\partial x_i^l} e_i^{kl}(\mathbf{x}^k, \mathbf{x}^l) \right|_{\mathbf{x}=\mathbf{x}^*}, \\ \hat{\kappa}_{ij}^{kl} &= \left. \frac{\partial}{\partial x_j^k} e_i^{kl}(\mathbf{x}^k, \mathbf{x}^l) \right|_{\mathbf{x}=\mathbf{x}^*}, \\ \kappa_{ij}^{kl} &= \left. \frac{\partial}{\partial x_j^l} e_i^{kl}(\mathbf{x}^k, \mathbf{x}^l) \right|_{\mathbf{x}=\mathbf{x}^*} \end{aligned} \quad (20)$$

with $i \neq j$.

Below, it will be useful to consider the exponent parameters that are related to the local per-capita net growth rates

$$W_i^k(\mathbf{X}^k) = \frac{G_i^k(\mathbf{X}^k) - M_i^k(\mathbf{X}^k)}{X_i^k}, \quad (21)$$

as these are a measure for patch quality. The exponent parameters related to these net growth rates can be expressed in terms of the already defined parameters as

$$\begin{aligned} \eta_i^+ &= \left. \frac{\partial W_i^{k+}}{\partial X_i^{k+}} \frac{X_i^{+*}}{W_i^{+*}} \right|_{\mathbf{X}=\mathbf{X}^*} = \frac{\alpha_{P_i}^+}{\alpha_{S_i}^+} (\phi_i^+ - \mu_i^+) + \phi_i^+ - 1, \\ \eta_i^- &= \left. \frac{\partial W_i^{k-}}{\partial X_i^{k-}} \frac{X_i^{-*}}{W_i^{-*}} \right|_{\mathbf{X}=\mathbf{X}^*} = \frac{\alpha_{P_i}^-}{\alpha_{S_i}^-} (\phi_i^- - \mu_i^-) - \mu_i^- - 1 \end{aligned} \quad (22)$$

for sources and sinks respectively.

Since the exponent parameters are derivatives of the logarithm of a function with respect to the logarithm of a population size, they give the power law exponent that characterizes the relationship between the function and the population size in the vicinity of the steady state. For instance, an exponent parameter of 1 describes a linear relationship. TABLE I summarizes all generalized parameters and their ecological interpretation.

Ecological considerations fix the sign or the possible range of exponent parameters. In particular, ϕ_i^k and μ_i^k must be positive since we expect local growth and mortality to increase with population size. In contrast, the local per capita net growth rate (21), can increase or decrease with density. The first situation is the Allee effect, which can occur at low densities when reduced opportunities for intraspecific interactions such as mating decrease survival. It is associated with $\eta_i^k > 0$. The opposite case, $\eta_i^k < 0$, is due to intraspecific competition. It induces a self-regulating negative feedback between net growth rate and population size which is stabilizing [29].

Different dispersal scenarios can be described by different conditions on $\hat{\omega}_i^{kl}$ and ω_i^{kl} : If dispersal is passive, we expect a fixed proportion of the population in the donor patch l to emigrate. Then the per-capita emigration rates are constant. In this case dispersal rates are

independent of the density in the recipient patch and linear in the density of the donor patch such that $\hat{\omega}_i^{kl} = 0$ and $\omega_i^{kl} = 1$. Other values of these exponent parameters describe adaptive or maladaptive dispersal: Usually it is expected that individuals disperse adaptively such that they increase their local per capita net growth rate, thus on average they should prefer sources over sinks. However, the local per capita net growth rate can decrease with density ($\eta_i^+ < 0$) even if $W_i^k(\mathbf{X}^k) > 0$, for instance if there is competition for a limited resource such as nesting sites or food. Then it might be favorable for part of the population to move from a source to a sink. In addition to this adaptive type of movement, maladaptive movement is also possible. In this case the per capita net growth rate decreases due to dispersal.

Here we consider two cases of maladaptive movement. First, if a source is subject to an Allee-effect ($\eta_i^+ > 0$) an increase in the source's population size also increases $W_i^k(\mathbf{X}^+)$. Then certainly movement is maladaptive if individuals additionally are more likely to leave ($\omega_i^{-+} > 1$, positive density dependence) or avoid to settle ($\hat{\omega}_i^{+-} < 0$) in the source when the source population size becomes larger. In this case, this can be called a perceived trap, since individuals falsely identify a high quality habitat as a bad one and avoid it [30, 31]. Second, if a sink is subject to competition ($\eta_i^- < 0$) an increase in its population size decreases $W_i^k(\mathbf{X}^-)$. Then movement certainly is maladaptive if individuals are more likely to settle ($\hat{\omega}_i^{+-} > 0$) or to stay ($\omega_i^{-+} < 1$, negative density dependence) in sinks when their sink population size is larger. In this case we have an ecological trap since individuals actively prefer to settle in a low quality habitat [32].

Finally we briefly discuss the meaning of generalized parameters for explicit modeling. A class of models is defined as all models that exhibit at least one steady state with the same set of generalized parameters. Thus the assumption of an existing steady state only requires that a class associated with the chosen set of generalized parameters contains at least one model. Such a model can always be found by choosing a suitable polynomial expression for the explicit functional forms. Hence if we vary values for exponent and scale parameters within a realistic range (see FIG. I) we are able to compare the stability of steady states of different model classes.

IV. ANALYTICAL RESULTS FOR ONE SPECIES

The reduced eigenvalue equation (8) becomes analytically solvable if only one species is present. This analytical solution provides a wealth of insights about the stability of the system, part of which we will derive in the following.

A. Eigenvalues of the Jacobian

There are two types of eigenvalues of the Jacobian. First, there are the eigenvalues that are obtained by solving (8) with $\alpha = \beta$ being the singular values of \mathbf{M} . Second, if the number of source patches M^+ is different from the number of sink patches M^- , there are the eigenvalues that are obtained by setting $\alpha = 0$ ($\beta = 0$) if $M^+ > M^-$ ($M^+ < M^-$) and solving (12), which takes for one species the simple form

$$P^k - d^k C^k = \lambda_0, \quad (23)$$

with $k = +$ if $M^+ > M^-$ and $k = -$ if $M^- > M^+$.

The reduced Jacobian in (8) that is obtained by setting $\alpha = \beta$ simplifies for one species to

$$\mathbf{j} = \begin{pmatrix} P^+ - d^+ C^+ & \beta \hat{C}^+ \\ \beta \hat{C}^- & P^- - d^- C^- \end{pmatrix} \quad (24)$$

with

$$P^+ = \alpha_P^+(\phi^+ - \mu^+) + \alpha_S^+ \phi^+ \quad (25)$$

$$P^- = \alpha_P^-(\phi^- - \mu^-) - q\alpha_S^+ \mu^- \quad (26)$$

$$C^+ = [\alpha_C^+(\omega^{-+} - \hat{\omega}^{+-}) + \alpha_S^+ \omega^{-+}]/d^+ \quad (27)$$

$$C^- = [q\alpha_C^+(\omega^{+-} - \hat{\omega}^{+-}) - q\alpha_S^+ \hat{\omega}^{+-}]/d^- \quad (28)$$

$$\hat{C}^+ = [\alpha_C^+(\omega^{+-} - \hat{\omega}^{+-}) - \alpha_S^+ \hat{\omega}^{+-}]/d^+ \quad (29)$$

$$\hat{C}^- = [q\alpha_C^+(\omega^{-+} - \hat{\omega}^{+-}) + q\alpha_S^+ \omega^{-+}]/d^- . \quad (30)$$

Since this is a 2×2 matrix, its eigenvalues are given by

$$\lambda_i = \frac{\text{tr}(\mathbf{j})}{2} \pm \sqrt{\frac{\text{tr}(\mathbf{j})^2}{4} - \det(\mathbf{j})}. \quad (31)$$

In our system, the trace of \mathbf{j} is

$$\begin{aligned} \text{tr}(\mathbf{j}) &= P^+ + P^- - d^+ C^+ - d^- C^- \\ &= \alpha_P^+(\phi^+ - \mu^+) + \alpha_P^-(\phi^- - \mu^-) \\ &\quad + \alpha_S^+(\phi^+ - \omega^{-+} + q\hat{\omega}^{+-} - q\mu^-) \\ &\quad + \alpha_C^+(\hat{\omega}^{+-} - \omega^{-+} + q\hat{\omega}^{+-} - q\omega^{+-}), \end{aligned} \quad (32)$$

and the determinant is

$$\det(\mathbf{j}) = (P^+ - d^+ C^+)(P^- - d^- C^-) - \beta^2 \hat{C}^+ \hat{C}^- . \quad (33)$$

The considered steady state is stable if the real part of both eigenvalues of the reduced Jacobian is negative and if the one-patch mode is stable, i.e., if $\text{tr}(\mathbf{j}) < 0$ and $\det(\mathbf{j}) > 0$ and if (see (23))

$$P^k - d^k C^k = \lambda_0 < 0, \quad (34)$$

with $k = +$ if $M^+ > M^-$ and $k = -$ if $M^- > M^+$.

In the absence of dispersal, the Jacobian has a diagonal form with the entries P^+ and P^- . The dispersal-dependent turnover rates α_S and α_C vanish. According to eqs. (25) and (26), both types of patches are stable if

$$\phi^+ < \mu^+, \quad \phi^- < \mu^-. \quad (35)$$

Parameter	Interpretation	realistic range
Turnover		
α_i^k	Total biomass turnover	> 0
$\alpha_{P_i}^k$	Purely local biomass turnover consisting of parts of local growth and mortality	> 0
$\alpha_{S_i}^k$	Biomass turnover due to source sink dynamics	≥ 0
$\alpha_{C_i}^k$	Biomass turnover due to pure dispersal dynamics	≥ 0
Scale		
ν_i^k	Fraction of local growth $G_i^k(\mathbf{x}^k)$ to total gain.	$[0,1]$
ρ_i^k	Fraction of local mortality $M_i^k(\mathbf{x}^k)$ to total loss.	$[0,1]$
$1 - \nu_i^k$	Fraction of immigration $\sum_l E_i^{kl}(\mathbf{x}^k, \mathbf{x}^l)$ to total gain.	$[0,1]$
$1 - \rho_i^k$	Fraction of emigration $\sum_l E_i^{lk}(\mathbf{x}^l, \mathbf{x}^k)$ to total loss.	$[0,1]$
ν_i^{kl}	Fraction of immigration $E_i^{kl}(\mathbf{x}^k, \mathbf{x}^l)$ along the link from l to k	$[0,1]$
ρ_i^{kl}	Fraction of emigration $E_i^{lk}(\mathbf{x}^l, \mathbf{x}^k)$ along the link from l to k	$[0,1]$
Exponent		
ϕ_i^k	Exponent of $G_i^k(\mathbf{x}^k)$ with respect to population i	$[0,2]$
$\phi_{i,j}^k$	Exponent of $G_i^k(\mathbf{x}^k)$ with respect to population j	$[0,2]$
μ_i^k	Exponent of $M_i^k(\mathbf{x}^k)$ with respect to population i	$[0,2]$
$\mu_{i,j}^k$	Exponent of $M_i^k(\mathbf{x}^k)$ with respect to population j	$[0,2]$
ω_i^{kl}	Exponent of $E_i^{kl}(\mathbf{x}^k, \mathbf{x}^l)$ with respect to population i in target patch k	$[-2,2]$
$\omega_{i,j}^{kl}$	Exponent of $E_i^{kl}(\mathbf{x}^k, \mathbf{x}^l)$ with respect to population i in starting patch l	$[-2,2]$
$\hat{\kappa}_{i,j}^{kl}$	Exponent $E_i^{kl}(\mathbf{x}^k, \mathbf{x}^l)$ with respect to population j in target patch k	$[-2,2]$
$\kappa_{i,j}^{kl}$	Exponent of $e_i^{kl}(\mathbf{x}^k, \mathbf{x}^l)$ with respect to population j in starting patch l	$[-2,2]$

TABLE I. Generalized parameters of species i and their ecological interpretation. The exponent parameters are elasticities of the respective function with respect to population sizes. $k = +, -$ is associated with either sources (+) or sinks (-).

In the following we refer to the term

$$\alpha_P^k(\phi^k - \mu^k) \quad (36)$$

as local feedback. If the local feedback in both patch types is negative, local dynamics exhibit a stable steady state because the local population is able to self regulate its size

B. When is a sufficiently large net source sink flow stabilizing?

First, we evaluate the conditions under which the net source-sink flow α_S^+ stabilizes the steady state for sufficiently large values. Since $q\alpha_S^+ = \alpha_S^-$ (see eq. (18)), both turnover rates are proportional to each other, and we can therefore focus on the effect of α_S^+ . For the sake of simplicity we assume that $\alpha_C^+ = 0$. If making α_S^+ arbitrarily large shall have a stabilizing effect, the trace of the reduced Jacobian \mathbf{j} must become negative and the determinant positive for sufficiently large α_S^+ . According to equations (32) and (33), the trace is linear in α_S^+ and the determinant is a quadratic function in α_S^+ . Further, the additional eigenvalue λ_0 in (34) must be negative for sufficiently large α_S^+ . Hence, the one-species source-sink dynamics are linearly stable for large α_S^+ if either

$$\omega^{-+} > \phi^+ \quad \text{if } M^+ > M^- \quad (37)$$

or

$$\mu^- > \hat{\omega}^{-+} \quad \text{if } M^- > M^+, \quad (38)$$

and

$$\frac{\partial \text{tr}(\mathbf{J})}{\partial \alpha_S^+} = \phi^+ - \omega^{-+} + q(\hat{\omega}^{-+} - \mu^-) < 0 \quad (39)$$

and

$$\begin{aligned} \frac{\partial^2 \det(\mathbf{J})}{\partial (\alpha_S^+)^2} = & q[(\phi^+ - \omega^{-+})(\hat{\omega}^{-+} - \mu^-) \\ & + \frac{\beta^2}{d^+d^-} \hat{\omega}^{-+} \omega^{-+}] > 0. \end{aligned} \quad (40)$$

The topology of the patch network affects stability only through the singular values β . Condition (40) has to be satisfied for all $\beta \in S$. For the special case that $M^+ = M^-$ there is no additional eigenvalue λ_0 and thus no condition (37) or (38).

If $\omega^{-+} < 0$, condition (37) cannot be satisfied. Further, conditions (38), (39) and (40) can not be satisfied simultaneously, hence we find:

A large net source-sink flow α_S^+ cannot stabilize the system if emigration and density in sources are negatively correlated, i.e., if $\omega^{-+} < 0$.

We therefore assume in the remainder of this section that $\omega^{-+} > 0$, and we identify several sets of conditions under which relations (37) to (40) can be satisfied for all $\beta \in S$.

Mainly two effects affect the stability of our metapopulation. First, if condition (37) resp. (38) is satisfied, an increasing net source-sink flow α_S^+ shifts the diagonal entries $P^k - d^k C^k$ of the respective patch type in the

Jacobian (4) to negative values. We call these diagonal entries intra-patch feedbacks since they indicate how the net growth rate of a population correlates with its local size. Negative intra-patch feedbacks are known to have a stabilizing influence [29, 33] because they indicate that a population is able to self regulate its population size. These intra-patch feedbacks are affected by the terms

$$\alpha_S^+(\phi^+ - \omega^{-+}) \quad \text{and} \quad q\alpha_S^+(\hat{\omega}^{-+} - \mu^-) \quad (41)$$

in sources and sink respectively, which means that they are *induced* by the net source-sink flow α_S . We therefore call the feedbacks with the prefactors (41) "induced intra-patch feedback".

Second, the sign of the term

$$\hat{\omega}^{-+}\omega^{-+} \quad (42)$$

reflects different types of feedback loops between the source and sink populations. Due to $\omega^{-+} > 0$ the sign of $\hat{\omega}^{-+}\omega^{-+}$ is identical to that of $\hat{\omega}^{-+}$. If $\hat{\omega}^{-+}\omega^{-+} < 0$, a perturbation to the source or sink population can trigger a positive feedback loop between the two types of patches if self regulation is weak: for instance, a positive perturbation to source populations increases immigration to sinks since $\omega^{-+} > 0$ and thus the population size of sinks. But because of $\hat{\omega}^{-+} < 0$ this also decreases emigration from sources and thus increases the source population further. If this positive inter-patch feedback is not opposed by sufficiently strong negative intra-patch feedbacks (41), it has a destabilizing effect. We explicitly excluded the effects of an increase of emigration from sources due to $\omega^{-+} > 0$ and a decrease of immigration in sinks due to $\hat{\omega}^{-+} < 0$ in this explanation since these effects pose intra-patch feedbacks which may suppress a positive feedback loop. By the same type of reasoning, the case $\hat{\omega}^{-+}\omega^{-+} > 0$ implies a negative inter-patch feedback, which has a stabilizing effect.

We obtain different stabilizing conditions depending on whether the net source-sink flow α_S^+ induces a negative intra-patch feedback in both or only one type of patches, i.e., whether (37) and (38) are both satisfied simultaneously or only one of them. In the first case, we can have either $\hat{\omega}^{-+}\hat{\omega}^{-+} > 0$ or $\hat{\omega}^{-+}\hat{\omega}^{-+} < 0$; in the second case we need $\hat{\omega}^{-+}\hat{\omega}^{-+} > 0$, i.e., we have a stabilizing negative inter-patch feedback loop.

1. Case I: the net source-sink flow induces negative intra-patch feedbacks and a negative inter-patch feedback loop

If conditions (37) and (38) are satisfied and additionally $\hat{\omega}^{-+} > 0$, the two intra-patch feedbacks are negative as well as the inter-patch feedback (see previous paragraph).

$\hat{\omega}^{-+} > 0$ means that condition (40) is satisfied for all β , and we need no further restrictions on the parameters. Thus the negative intra-patch feedbacks (41) induced by α_S are sufficient for stabilization. In particu-

lar condition (38) assures that the positive effect of immigration on sink population growth is limited by the density-dependent increase in mortality for population sizes above the steady state. A large enough net source-sink flow α_S^+ can thus potentially stabilize a sink that would be unstable otherwise. This is the well-known rescue effect [34, 35]. We can summarize the first result as follows:

I A sufficiently large net source-sink flow α_S^+ stabilizes source-sink dynamics if it induces a negative intra-patch feedback in all patches ($\phi^+ < \omega^{-+}$ and $\hat{\omega}^{-+} < \mu^-$) and a negative inter-patch feedback, hence immigration and population size in sinks are positively correlated ($\omega^{-+}\hat{\omega}^{-+} > 0$).

2. Case II: the net source-sink flow induces negative intra-patch feedbacks and potentially a positive inter-patch feedback loop

For our second case, conditions (37) and (38) again are satisfied, but now $\hat{\omega}^{-+} < 0$. This means that condition (40) has a negative last term, the absolute value of which is largest for $\beta^2 = d^+d^-$. Condition (40) can be rewritten in this case as a condition for $|\hat{\omega}^{-+}|$,

$$|\hat{\omega}^{-+}| < \mu^- \left(\frac{\omega^{-+}}{\phi^+} - 1 \right) \quad (43)$$

which must be satisfied for stability. Otherwise a detrimental positive feedback loop is present. Our second result is therefore:

II If immigration and population size in sinks are negatively correlated ($\omega^{-+}\hat{\omega}^{-+} < 0$), an increase in α_S^+ can still stabilize source-sink dynamics if it induces a negative intra-patch feedback in all patches ($\phi^+ < \omega^{-+}$ and $\hat{\omega}^{-+} < \mu^-$), which has to be strong enough to suppress a positive feedback loop between source and sink populations which is the case if eq. (43) is satisfied.

3. Case III: the net source-sink flow induces a positive intra-patch feedback in one type and a negative one in the other

Now we consider the case that only one of the conditions (37) and (38) is satisfied. In this case (40) can only be satisfied if $\hat{\omega}^{-+} > 0$, since we have established above that $\omega^{-+} > 0$. If we denote with β_0 the smallest value of all $\beta \in S$, condition (40) now becomes

$$|(\phi^+ - \omega^{-+})(\hat{\omega}^{-+} - \mu^-)| < \frac{\beta_0^2}{d^+d^-} \hat{\omega}^{-+}\omega^{-+}. \quad (44)$$

Furthermore, condition (39) becomes

$$\frac{|\phi^+ - \omega^{-+}|}{|\hat{\omega}^{-+} - \mu^-|} \geq q \quad \text{if } M^- \leq M^+. \quad (45)$$

In both cases the less numerous patch type has a positive diagonal entry in the Jacobian when the net source-sink flow α_S^+ is large. There a positive intra-patch feedback (41) is induced which has to be smaller than the negative intra-patch feedback which is induced in the more numerous patch (see (45)). As discussed before this is destabilizing due to a non-local demographic Allee-effect. This destabilizing effect can be countered by a negative feedback loop (or negative inter-patch feedback) between source and sink populations due to the choice $\omega^{-+}\hat{\omega}^{-+} > 0$. The induced feedback loop has to be strong enough to suppress the demographic Allee-effect, which is reflected by the term $\hat{\omega}^{-+}\omega^{-+}$ on the right-hand side of condition (44). This leads to our third result:

III A large net source-sink flow α_S^+ can stabilize source-sink dynamics even when it induces a positive intra-patch feedback in the less numerous patch type ($\phi^+ > \omega^{-+}$ or $\hat{\omega}^{-+} > \mu^-$), which has to be smaller than the induced negative intra-patch feedback in the other type, see eq. (45). In this case α_S must also induce a sufficiently strong negative feedback loop between source and sink populations ($\omega^{-+}\hat{\omega}^{-+} > 0$) to overcome demographic Allee-effects, see eq. (44)

C. When is net source-sink flow stabilizing for some intermediate range of values?

In the following, we will consider the case that there is an unstable steady state at $\alpha_S^+ = 0$ and at $\alpha_S^+ \rightarrow \infty$, and we will demonstrate that there can be an intermediate interval of values of the net source-sink flow α_S^+ for which the dynamics are stable. We will explicitly give three examples of parameter sets which satisfy the conditions for stability. Again we assume that $\alpha_C^+ = 0$ for the sake of simplicity. We write the determinant (33) as

$$\det(\alpha_S^+) = A(\beta^2)(\alpha_S^+)^2 + B\alpha_S^+ + C \quad (46)$$

and the trace (32) as

$$\text{tr}(\alpha_S^+) = D\alpha_S^+ + E, \quad (47)$$

which means that

$$A(\beta^2) = q[(\phi^+ - \omega^{-+})(\hat{\omega}^{-+} - \mu^-) + \frac{\beta^2}{d^+d^-}\omega^{-+}\hat{\omega}^{-+}] \quad (48)$$

$$B = \alpha_P^-(\phi^+ - \omega^{-+})(\phi^- - \mu^-) + q\alpha_P^+(\hat{\omega}^{-+} - \mu^-)(\phi^+ - \mu^+) \quad (49)$$

$$C = \alpha_P^+\alpha_P^-(\phi^+ - \mu^+)(\phi^- - \mu^-) \quad (50)$$

$$D = \phi^+ - \omega^{-+} + q(\hat{\omega}^{-+} - \mu^-) \quad (51)$$

$$E = \alpha_P^+(\phi^+ - \mu^+) + \alpha_P^-(\phi^- - \mu^-). \quad (52)$$

If the steady state shall be unstable when dispersal is absent ($\alpha_S^+ = 0$), at least one local feedback must be positive, thus either $\phi^+ - \mu^+ < 0$ or $\phi^- - \mu^- < 0$ must be violated (see eq. (35)). Further, if the steady state shall be unstable for large α_S^+ , condition (39) ($D < 0$) or condition (40) ($A(\beta^2) > 0$) or both must be violated. Here we focus on the violation of (40) and assume that $A(\beta^2) < 0$ for at least one $\beta \in S$. (In fact, if $A(\beta^2) > 0$ for all $\beta \in S$, the conditions required to obtain an intermediate range of stability appear difficult to satisfy, as a numerical exploration of selected parameter combinations did not yield any positive results.)

Now, a straightforward way of obtaining a range of α_S^+ values outside of which the system is unstable is when the determinant (33) has two positive roots, so that the determinant is positive within and negative outside these two roots. This means that $B > 0$ and $C < 0$ (see FIG. 2 (a)). If an intermediate region shall be stable, the determinant has to be positive for all $\beta \in S$ within this region. Since β enters the determinant only via A , the determinant is positive for all $\beta \in S$ in the intermediate region if it is positive for the value β^2 for which $A(\beta^2)$ is minimal.

Which value of β^2 minimizes A , depends on the sign of $\hat{\omega}^{-+}\omega^{-+}$ (see (48)),

$$\beta^2 = \begin{cases} d^+d^- & \text{if } \hat{\omega}^{-+}\omega^{-+} < 0 \\ \beta_0^2 & \text{if } \hat{\omega}^{-+}\omega^{-+} \geq 0. \end{cases} \quad (53)$$

We assume in the following for simplicity that the lowest singular value is $\beta_0 = 0$. The conditions for stability that we will find with this assumption are sufficient conditions. The parameter regions that show stability can therefore be somewhat larger than the ones calculated by us.

Besides the conditions $B > 0$, $C < 0$ and $A < 0$ for at least one β , we additionally require the condition

$$B^2 - 4AC > 0 \quad (54)$$

in order to obtain two positive roots of the determinant (46). Let us write the expression (49) as $B = B_1 + B_2$. In the case $\beta = 0$ we have $B^2 - 4AC = (B_1 - B_2)^2 > 0$ such that we need no further constraints on A , B and C . If $\beta > 0$, the condition $B^2 - 4AC > 0$ is still satisfied if $\hat{\omega}^{-+}\omega^{-+} \geq 0$. But if $\hat{\omega}^{-+}\omega^{-+} < 0$ (in which case $\beta^2 = d^+d^-$ minimizes $A(\beta)$, see (53)), the requirement that $B^2 - 4AC > 0$ must be met explicitly. We rewrite this condition (setting $\beta^2 = d^+d^-$) as

$$(B_1 - B_2)^2 > 4|C||\hat{\omega}^{-+}\omega^{-+}|. \quad (55)$$

A comparison with the explicit expressions for B_1 and B_2 in (49) shows that this inequality can be satisfied by increasing α_P^- or α_P^+ or q or $|\phi^+ - \mu^+|$ or $|\phi^- - \mu^-|$ sufficiently far while keeping the signs of the other terms A to E fixed. One of these possibilities will always be available without violating the conditions imposed on the signs of the terms or the other conditions for stability. This will be clear when looking at the examples below.

If the model shall be stable between the two roots of the determinant, we have to satisfy two more conditions, namely that the trace (47) and the additional eigenvalue given by (34) are negative. In order to specify constraints on the parameters that ensure these conditions, it is useful to define the source's and sink's resistances R_S^+ and R_S^- to changes in the net-source sink flow α_S^+ as

$$R_S^+ = -\alpha_P^+ \frac{\phi^+ - \mu^+}{\phi^+ - \omega^{-+}}, \quad R_S^- = -\frac{\alpha_P^-}{q} \frac{\phi^- - \mu^-}{\hat{\omega}^{-+} - \mu^-}. \quad (56)$$

They are the roots of the determinant (46) for $\beta_0^2 = 0$ if the above-mentioned conditions ($A < 0$, $B > 0$, $C < 0$) are satisfied. In two of our three examples below, we will have $\hat{\omega}^{-+}\omega^{-+} > 0$ such that $\beta^2 = 0$ minimizes A , and R_S^+ and R_S^- are the two values of α_S^+ that delimit the stable region.

The additional eigenvalue given by (34) is

$$\lambda_0 = \begin{cases} \alpha_S^+(\phi^+ - \omega^{-+}) + \alpha_P^+(\phi^+ - \mu^+) & \text{if } M^+ > M^- \\ \alpha_S^+q(\hat{\omega}^{-+} - \mu^-) + \alpha_P^-(\phi^- - \mu^-) & \text{if } M^- > M^+. \end{cases} \quad (57)$$

Both expressions are linear in α_S^+ and go through zero for $\alpha_S^+ = R_S^+$ if $M^+ > M^-$ and for $\alpha_S^+ = R_S^-$ if $M^+ < M^-$. A larger resistance therefore means that the value of α_S^+ required to change the sign of λ_0 is larger, i.e., the stability (or instability) of the uncoupled (i.e. $\alpha_S^+ = 0$) system is more resistant to an increase of α_S^+ . (And a negative value of the resistance means that an increase of α_S^+ cannot change the sign of λ_0 at all since α_S^+ cannot be negative.)

The following three examples are chosen such that, by fixing the signs of the slope and intercepts of the additional eigenvalue, we can make sure that λ_0 is negative between the two roots of the determinant. Similarly, by fixing the signs of D and E in the trace (47) of the Jacobian, we can make sure that it is negative between the two roots of the determinant. For the first two examples the net source-sink flow α_S^+ induces intra-patch feedbacks (41) with opposite signs. For the third example it induces a negative intra-patch feedbacks in both patch types. Then the destabilization for large α_S^+ occurs due to a positive feedback loop ($\hat{\omega}^{-+}\omega^{-+} < 0$).

1. Case IV: the net source-sink flow induces intra-patch feedbacks with opposite signs

An example for how the conditions $A(\beta^2) < 0$, $B > 0$, $C < 0$, and (54) can be satisfied is given by $\phi^+ - \mu^+ < 0$, $\phi^- - \mu^- > 0$, $\phi^+ - \omega^{-+} > 0$, $q(\hat{\omega}^{-+} - \mu^-) < 0$, $R_S^+ > R_S^-$, and $\hat{\omega}^{-+}\omega^{-+} \geq 0$. According to (48) A is minimal if $\beta^2 = \beta_0^2 = 0$. If we compare the choice of parameters with the expressions (48) to (52), it is straightforward to see that $A(0) < 0$, $B > 0$, $C < 0$, thus fulfilling the condition that the determinant with $\beta^2 = 0$ has two positive roots, between which all determinants are positive.

The additional eigenvalue (57) is negative between the two roots R_S^+ and R_S^- due to the requirement $R_S^+ > R_S^-$, regardless of the choice of M^+ and M^- . This situation is illustrated in FIG. 2 (b).

Finally we have to show that the trace (47) is negative between R_S^+ and R_S^- . We start with $R_S^- < R_S^+$ and transform this inequality,

$$\begin{aligned} \frac{-\alpha_P^-(\phi^- - \mu^-)}{q(\hat{\omega}^{-+} - \mu^-)} &< \frac{-\alpha_P^+(\phi^+ - \mu^+)}{\phi^+ - \omega^{-+}} \\ -\frac{\alpha_P^-(\phi^- - \mu^-) + \alpha_P^+(\phi^+ - \mu^+)}{q(\hat{\omega}^{-+} - \mu^-) + (\phi^+ - \omega^{-+})} &< \frac{-\alpha_P^-(\phi^- - \mu^-)}{q(\hat{\omega}^{-+} - \mu^-)}. \end{aligned} \quad (58)$$

The left-hand side in the last line is the root of the trace (47) and the right-hand side is the lower root of the determinant (46). With the choice $D < 0$ we have made sure that the trace is negative between the two roots of the determinant (see FIG. 2 (b)).

Our second example is obtained by exchanging the sources and sinks in the first example. This means that $\phi^+ - \mu^+ > 0$, $\phi^- - \mu^- < 0$, $\phi^+ - \omega^{-+} < 0$, $q(\hat{\omega}^{-+} - \mu^-) > 0$, $R_S^+ < R_S^-$, and $\hat{\omega}^{-+}\omega^{-+} \geq 0$. Additionally, we choose again $D < 0$ and obtain by a calculation similar to (58) that the root of the trace is smaller than the smaller of the two roots of the determinant, which is now R_S^+ .

We can summarize the two examples as follows:

IV The net source-sink flow α_S^+ can stabilize the system for an intermediate range of values if the resistance $R_S^{k_1}$ of the patch type k_1 with a negative local feedback $\alpha_P^{k_1}(\phi^{k_1} - \mu^{k_1})$ is larger than the resistance $R_S^{k_2}$ of the other patch type k_2 with a positive local feedback $\alpha_P^{k_2}(\phi^{k_2} - \mu^{k_2})$. Further it is required that an increasing α_S^+ induces a positive intra-patch feedback (41) in the former and a negative intra-patch feedback in the latter. Stability is given for net source-sink flows between both resistances ($R_S^{k_2} < \alpha_S^+ < R_S^{k_1}$).

2. Case V: the net source-sink flow induces negative intra-patch feedbacks in both patch types and a positive feedback loop between source and sink populations

The third example is given by $\phi^+ - \mu^+ > 0$, $\phi^- - \mu^- < 0$, $\phi^+ - \omega^{-+} < 0$, $q(\hat{\omega}^{-+} - \mu^-) < 0$, $-R_S^+ < R_S^-$, and $\hat{\omega}^{-+}\omega^{-+} < 0$, which implies $\hat{\omega}^{-+} < 0$. Now an increasing net source-sink flow α_S^+ induces a negative intra-patch feedback (41) for both types of patches. Now we find according to (2) that $A(\beta^2) < 0$ is minimal if $\beta^2 = d^+d^-$, implying

$$|\hat{\omega}^{-+}| > \mu^- \left(\frac{\omega^{-+}}{\phi^+} - 1 \right). \quad (59)$$

The above choice of parameters satisfies $C < 0$ and $D < 0$ for the expressions (50) and (51). The condition $B > 0$

for the expression (49) is also satisfied since $R_S^+ < R_S^-$. Condition (55) can be satisfied without conflict with the other conditions by making α_P^- or $|\phi^- - \mu^-|$ large enough. In this way, we will additionally achieve that E is negative, such that the trace (47) of the reduced Jacobian (12) is always negative. The final condition that we need to satisfy is a negative additional eigenvalue (57) between the two roots of the determinant. For $M^+ < M^-$, the eigenvalue λ_0 is negative for all α_S^+ . For $M^+ > M^-$, it becomes negative for $\alpha_S^+ > R_S^+$. Now, from FIG. 2 (a) we can conclude that the two roots of the determinant with $\beta^2 = d^+d^-$ both are to the right-hand side of R_S^+ . For $\beta^2 = 0$, we have $A > 0$ and the determinant is a parabola that opens upwards and has its larger root at R_S^+ . For $\beta^2 = d^+d^-$, the curvature becomes negative, which means that the two roots of the determinant must lie to the right of R_S^+ . An analogous calculation can be done if $\phi^+ - \mu^+ < 0$, $\phi^- - \mu^- > 0$, and $-R_S^+ > R_S^-$.

In summary:

V If the net source-sink flow α_S^+ induces a stabilizing negative intra-patch feedback in both sources and sinks ($\phi^+ - \omega^{-+} < 0$ and $q(\hat{\omega}^{-+} - \mu^-) < 0$), an intermediate range of stability is possible if α_S^+ also induces a destabilizing positive feedback loop for larger values ($\hat{\omega}^{-+}\omega^{-+} < 0$), which has to dominate the induced negative intra-patch feedbacks (see eq. (59)). It is required that one patch type needs

to have a positive local feedback ($\phi^k > \mu^k$), while the other needs to have a negative one ($\phi^- < \mu^-$), with the absolute value of the former's resistance being smaller than the latter's ($-R_S^+ < R_S^-$).

D. When is dispersal turnover stabilizing?

Next, we analyze the conditions under which either a sufficiently large or an intermediate dispersal turnover α_C^+ stabilizes the system. Proceeding similarly as before, we write the trace (32) and the determinant (33) as functions of α_C^+ ,

$$\det(\alpha_C^+) = A_C(\beta^2)(\alpha_C^+)^2 + B_C(\beta^2)\alpha_C^+ + C_C(\beta^2) \quad (60)$$

and

$$\text{tr}(\alpha_C^+) = D_C\alpha_C^+ + E_C. \quad (61)$$

All three coefficients in the determinant depend on β^2 if the net source-sink flow α_S^+ does not vanish.

1. Case VI: large dispersal turnover stabilizes the system

If the source-sink dynamics shall be stable for $\alpha_C^+ \rightarrow \infty$, we require $D_C < 0$ and $A_C(\beta^2) > 0$ for $\beta \in S$. Further the additional eigenvalue

$$\lambda_0 = \begin{cases} \alpha_C^+(\hat{\omega}^{-+} - \omega^{+-}) + \alpha_S^+(\phi^+ - \omega^{-+}) + \alpha_P^+(\phi^+ - \mu^+) & \text{if } M^+ > M^- \\ \alpha_C^+q(\hat{\omega}^{+-} - \omega^{-+}) + \alpha_S^+q(\hat{\omega}^{-+} - \mu^-) + \alpha_P^-(\phi^- - \mu^-) & \text{if } M^- > M^+ \end{cases} \quad (62)$$

given by (34) must become negative for large α_C^+ . From the first two requirements

$$A_C(\beta^2) = q(\hat{\omega}^{+-} - \omega^{-+})(\hat{\omega}^{-+} - \omega^{+-})\left(1 - \frac{\beta^2}{d^+d^-}\right) > 0 \quad (63)$$

and

$$D_C = \hat{\omega}^{+-} - \omega^{-+} + q(\hat{\omega}^{-+} - \omega^{+-}) < 0 \quad (64)$$

we find that

$$\begin{aligned} \omega^{-+} &> \hat{\omega}^{+-} \\ \omega^{+-} &> \hat{\omega}^{-+}. \end{aligned} \quad (65)$$

for all $\beta^2 < d^+d^-$. For $\beta^2 = d^+d^-$ we have $A_C = 0$, and the sign of the determinant for large α_C^+ is not determined by A_C but by B_C . We therefore have to add the condition $B_C(d^+d^-) > 0$. To evaluate this condition further, we define again the resistances of sources and sinks R_C^+ and

R_C^- as

$$\begin{aligned} R_C^+ &= -\frac{\alpha_P^+(\phi^+ - \mu^+) + \alpha_S^+\phi^+}{\hat{\omega}^{+-} - \omega^{-+}}, \\ R_C^- &= -\frac{\alpha_P^-(\phi^- - \mu^-) - q\alpha_S^+\mu^-}{q(\hat{\omega}^{-+} - \omega^{+-})}. \end{aligned} \quad (66)$$

These are identical to the roots of the determinant for $\beta^2 = 0$. Compared to the resistances to the net source-sink flow (56), the denominators are replaced by the dispersal-induced intra-patch feedbacks $\alpha_C^+(\hat{\omega}^{+-} - \omega^{-+})$ in sources and $q\alpha_C^+(\hat{\omega}^{-+} - \omega^{+-})$ in sinks. The numerators

$$\alpha_P^-(\phi^- - \mu^-) - q\alpha_S^+\mu^- \quad \text{and} \quad \alpha_P^+(\phi^+ - \mu^+) + \alpha_S^+\phi^+ \quad (67)$$

represent extended local feedbacks, which have an additional term due to source-sink dynamics. From

$$\begin{aligned} B_C(0) &= (\hat{\omega}^{+-} - \omega^{-+})[\alpha_P^-(\phi^- - \mu^-) - q\alpha_S^+\mu^-] \\ &\quad + q(\hat{\omega}^{-+} - \omega^{+-})[\alpha_P^+(\phi^+ - \mu^+) + \alpha_S^+\phi^+] > 0 \end{aligned} \quad (68)$$

follows that stability for large α_C^+ is only possible if the extended local feedback is negative for at least one type

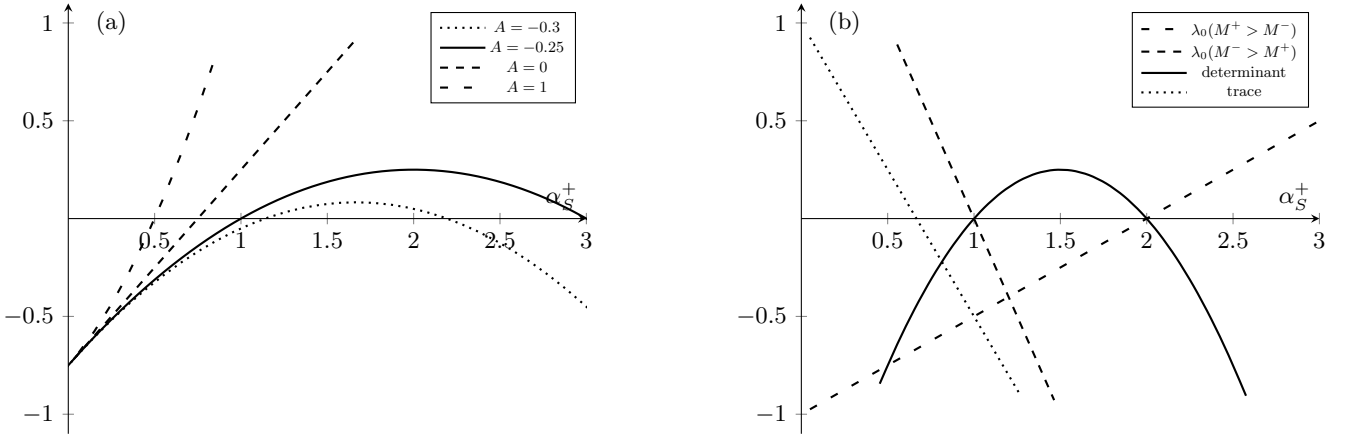


FIG. 2. Parabolas with $Ax^2 + x - 0.75$, thus $B > 0$, $C < 0$, and with varying A (a). The region between the two roots (if they exist) is positive for a fixed $A_0 < 0$ and all parabolas with $A > A_0$ are positive too within that region, even when $A > 0$. Determinant, trace, and additional eigenvalues (57) depending on the relation of numbers of sources (M^+) and sinks (M^-) for the parameter choice of the first example with $\phi^+ - \mu^+ < 0$, $\phi^- - \mu^- > 0$, $\phi^+ - \omega^{+-} > 0$, $q(\hat{\omega}^{+-} - \mu^-) < 0$, $R_S^+ > R_S^-$, and $\hat{\omega}^{-+}\omega^{-+} \geq 0$ (b). The trace and additional eigenvalues are always negative between the determinants roots.

of patches. If both patches have a negative extended local feedback, the system is already stable for $\alpha_C^+ = 0$ according to (35), thus an increase of dispersal turnover has no effect on stability.

More interesting is the case where the extended local feedbacks (67) have opposite signs, since then the system is unstable for $\alpha_C^+ = 0$. We obtain the result:

VI A large dispersal turnover α_C^+ is stabilizing if it induces a negative intra-patch feedback (65) in both patch types and if their extended local feedbacks (67) have opposite signs. Additionally, the absolute value of the resistance of the patch type with a negative extended local feedback has to be larger than the absolute value of the resistance of the other, see (68).

2. Case VII: intermediate dispersal turnover stabilizes the system

To find an intermediate region of stability we follow the same approach as for α_S^+ . We set $\alpha_S^+ = 0$ for the sake of simplicity. This means that the coefficients B_C and C_C are now independent of β^2 . As in the previous subsection we assume that $A_C(\beta^2) < 0$ for at least one $\beta \in S$, $B_C > 0$, and $C_C < 0$. From the expression (63) we can deduce that $A_C(\beta^2) < 0$ is actually fulfilled for all $\beta^2 \neq d^+d^-$ if the induced intra-patch feedbacks have opposite signs, i.e., if one of the two conditions (65) is satisfied while the other is violated. For $\beta^2 = d^+d^-$ the determinant is a linear function of α_C^+ with a positive slope, and its root is smaller than all roots of determinants with smaller β^2 (see FIG. 2 (a)). The intermediate region of stability is again bounded by the roots of the determinant with a

minimal $A_C(\beta^2)$, and we therefore focus on the situation $\beta = \beta_0$. From

$$C_C = [\alpha_P^+(\phi^+ - \mu^+)][\alpha_P^-(\phi^- - \mu^-)] < 0 \quad (69)$$

we conclude that the local feedback (36) of sources and sinks have opposite signs. Then the assumption $B_C > 0$ requires that the induced intra-patch feedback ($\alpha_C^+(\hat{\omega}^{+-} - \omega^{+-})$ and $q\alpha_C^+(\hat{\omega}^{+-} - \omega^{+-})$) and the local feedback (36) need to have opposite signs for each patch type respectively. We further note that the roots of the determinant only exist if

$$B_C^2 - 4A_C C_C > 0. \quad (70)$$

Since the resistances R_C^+ and R_C^- are the absolute values of the determinants roots, the additional eigenvalue (62) is negative between the roots if we further require that the resistance of the patch with a positive local feedback (36) is lower than the resistance of the other patch type (see also FIG. 2 (b)). Then the intermediate region of stability is bounded by the resistances, regardless of the value of β_0 (see FIG. 2 (a)).

Hence we can formulate our last result:

VII The dispersal turnover α_C can stabilize the system for an intermediate range of values if the resistance $R_C^{k_1}$ given by (66) of the patch type k_1 with a negative local feedback $\alpha_P^{k_1}(\phi^{k_1} - \mu^{k_1})$ is larger than the resistance $R_C^{k_2}$ of the other patch type k_2 with a positive local feedback $\alpha_P^{k_2}(\phi^{k_2} - \mu^{k_2})$. Further it is required that an increasing α_C^+ induces a positive intra-patch feedback ($\hat{\omega}^{+-} - \omega^{+-}$ or $\hat{\omega}^{-+} - \omega^{-+}$) in the former and a negative intra-patch feedback in the latter.

E. Maladaptive dispersal can be stabilizing

In the previous sections we found various conditions for the stabilizing effect of dispersal between sources and sinks. For instance the conditions (37) to (40) show that large net source-sink flows α_S^+ can have a stabilizing effect independently of the sign of the local feedback $\alpha_P^k(\phi^k - \mu^k)$ (and hence independent of local dynamics in general) and over a wide range of the dispersal-related exponent parameters. These conditions are so general that they include instances of maladaptive dispersal. As explained in section III, perceptual traps are characterized by superlinear emigration from sources ($\omega^{-+} > 1$), combined with a positive exponent of the local per capita net growth rate ($\eta^+ > 0$). We find from section IV B that there always exists a threshold value of α_S^+ above which the system is stable irrespective of the sign of local feedbacks and as long as conditions (37) to (40) are satisfied, even for perceptual traps. The same is true for ecological traps which were characterized by a positive correlation of population size in sinks and immigration rates ($\hat{\omega}^{-+} > 0$) in combination with a negative exponent of the local per capita net growth rate ($\eta^- < 0$).

There also exist intermediate ranges of α_S^+ for which stabilization is possible if a trap is present. For instance the choice of parameters according to the second example in section IV C with $\phi^+ - \mu^+ > 0$, $\phi^- - \mu^- < 0$, $\phi^+ - \omega^{-+} < 0$, $q(\hat{\omega}^{-+} - \mu^-) > 0$, $R_S^+ < R_S^-$, and $\hat{\omega}^{-+}\omega^{-+} \geq 0$ promotes stability. Further we can choose $\phi^+ > 1$ (such that $\eta^+ > 0$) and $\omega^{-+} > 1$ without violating this choice of parameters, thus obtaining stabilization of a perceptual trap. Additionally we can choose $\hat{\omega}^{-+} > 0$, such that an ecological trap may be stable ($\eta^- < 0$ regardless of the choice of μ^-). Stabilization is even possible if both types of traps are present simultaneously.

Even in cases where maladaptive dynamics cannot be stabilized by increasing the net source-sink flow alone, they can be stabilized by an additional dispersal turnover α_C^+ if it induces a negative intra-patch feedback in the appropriate patch type, which is the case if $0 < \hat{\omega}^{-+} < \omega^{+-}$ and $\hat{\omega}^{+-} < 1 < \omega^{-+}$ according to condition (65).

A stabilization of a perceptual trap is possible in general because the source population which is subject to a local Allee-effect ($\eta^+ > 0$) is limited by strong emigration due to a high exponent of emigration ($1 < \omega^{-+}$).

V. NUMERICAL RESULTS AND LARGER FOOD WEBS

To confirm the analytical results and to check how these translate to metacommunities with more species we performed numerical analysis for varying net source-sink flow α_S^+ and dispersal turnover α_C^+ . For each set of exponent and scale parameters, we generated an ensemble of 100.000.000 biregular systems with variable patch numbers drawn uniformly from 10 to 25. We com-

pare systems with only one species with metacommunities with $N = 10$ species. These metacommunities were generated using the niche model [36] in which the number of links are drawn using a beta distribution such that a mean connectance of $C = 0.1$ results. The link strength l_{ij} for existing links was drawn from a narrow gaussian distribution with mean value 0 and a 10% coefficient of variation. This allows us to define the inter-specific exponent parameters as $\phi_{ij}^k = \mu_j^k |l_{ij}| / \sum_{n=1}^N |l_{in}|$ and $\mu_{ij}^k = \phi_j^k |l_{ij}| / \sum_{n=1}^N |l_{nj}|$ such that the exponent of growth (loss) of species i is proportional to the exponent of loss (growth) of species j with a prey (predator) centric normalization of the link strength. Further we employ allometric scaling [37, 38] for the local turnover rates $\alpha_{P_i}^k = 10^{-2n_i}$. We chose $q = 1$ for simplicity. Other values of q shifted the transition lines, but the qualitative results were not influenced by q .

Within these ensembles, we evaluated the proportion of stable webs, see FIG. 3, in dependence of the normalized turnover rates $\alpha_{S_i}^+ / \alpha_i^k$ (with $\alpha_{C_i}^+ = 0$) or $\alpha_{C_i}^+ / \alpha_i^k$ (with $\alpha_{S_i}^+ = 0$), with

$$\alpha_i^k = \alpha_{P_i}^k + \alpha_{S_i}^k + \alpha_{C_i}^k. \quad (71)$$

The second parameter that we varied is either ω_i^{+-} or $\hat{\omega}_i^{+-}$. For the metacommunities these parameters were varied for exactly one species. All other parameters were fixed to the values given in TABLE II. Our parameter choices were such that the stability criteria I to VII found in the previous section can be indicated easily in the plots. Each stability criterion is marked in the plots, indicated by different parameter ranges. The analytical transitions calculated for a single population are marked for larger metacommunities ($N = 10$) as well, such that we can compare if the analytically found results for one species still hold true for larger foodwebs.

FIG. 3 (a) shows that stabilisation occurs for large net source-sink flows α_S^+ if $-1/2 < \hat{\omega}_i^{-+} < 1$. Then the net source-sink flow induces a negative intra-patch feedback in both patch types ($\phi^+ < \omega^{-+}$ and $\hat{\omega}^{-+} < \mu^-$, see (37) and (38)). For $-1/2 < \hat{\omega}_i^{-+} < 0$ condition (43) is satisfied such that a positive feedback loop ($\omega^{-+}\hat{\omega}^{-+} < 0$) is suppressed, which corresponds to result II. For $0 < \hat{\omega}_i^{-+} < 1$ stabilisation for large α_S^+ corresponds to result I. Here no suppression of a feedback loop is needed since $\omega^{-+}\hat{\omega}^{-+} > 0$. For $1 < \hat{\omega}^{-+} < 3/2$ we find two stable regimes depending on the number of patches. If the sources are more numerous ($M^+ > M^-$) the net source-sink flow stabilizes for large values corresponding to result III. In that case only condition (37) has to be satisfied. Here the generated webs with $M^+ < M^-$ can not be stable for large α_S^+ since condition (38) can not be satisfied. In that case a stabilization occurs for intermediate values, which corresponds to result IV. The stable regions are limited by the determinant's roots, which coincide with the resistances R_S^+ and R_S^- (yellow lines) for $\beta_0 = 0$. We observe that stabilization below the resistance $\alpha_S^+ < R_S^+$ (marked as X) is possible for

FIG. 3	ϕ_i^+	μ_i^+	ϕ_i^-	μ_i^-	ω_i^{-+}	$\hat{\omega}_i^{-+}$	ω_i^{+-}	$\hat{\omega}_i^{+-}$	$\alpha_{P_i}^+/\alpha_{P_i}^-$	$\alpha_{P_i}^+/\alpha_i^+$
(a) and (b)	1	1/2	1/2	1	3/2	1/2	0	0	1	0.1
(c) and (d)	0.75	0.7	1/4	1/2	1.75	-1/2	0	0	3	0.1
(e) and (f)	1/2	1	2	1	1.75	-1	0	0	1	0.1
(g) and (h)	1	2	2	1	1.75	1/2	2	1	1	0.1

TABLE II. Parameter values of exponent parameters and turnover rates used in the plots in figures 3 (a) to 3 (h) for metapopulations ((a), (c), (e), and (g)) and metacommunities with $N = 10$ ((b), (d), (f), and (h)). The last column shows the ratio of the local turnover to the total turnover $\alpha_{P_i}^+/\alpha_i^+$, which is only relevant for the species within the respective metacommunity for which no turnover rates are varied.

$\omega^{-+}\hat{\omega}^{-+} > 0$ if $\beta_0 > 0$, which is a situation for which we did not perform an analytical calculation. This region is limited by the determinant's roots with $\beta_0 = d^+d^-$ (blue line).

For the metapopulation shown in FIG. 3 (c), stabilization for large net source-sink flows occurs for $\omega^{-+} > 1.5$ corresponding to result II. An intermediate region of stability can be found for $1.06 < \omega^{-+} < 1.5$ corresponding to result V. Destabilization for large values occurs because of a positive feedback loop ($\omega^{-+}\hat{\omega}^{-+} < 0$). The stable region is then limited by the determinant's roots with $\beta_0 = d^+d^-$.

In FIG. 3 (e), stabilization occurs for large α_S^+ if $\omega^{-+} > 1$, which corresponds to result II. Further we observe intermediate ranges of stability for $-1 < \omega^{-+} < 1$, which correspond to result IV. We additionally find less stable regions for $\omega^{-+} < 0$, which correspond to the fact that the number of patches of each type influences the stability through β_0 . The resistances (yellow lines) act as a transition line only if the corresponding patch type is more numerous. Otherwise, extended regions of stability exist for either $M^+ > M^-$ and $M^- > M^+$ which are bounded by the determinant's (blue line) or trace's root (magenta line).

For the metapopulation shown in FIG. 3 (g), the dispersal turnover is stabilizing for large values if it induces a negative intra-patch feedback in both patch types (see (65)), which corresponds to result VI. This is the case if $\omega^{-+} > 1$. Further an intermediate region of stability exists if $-0.5 < \omega^{-+} < 1$, corresponding to result VII. Again we find extended regions of lower stability if the number of patches of each type are not equal (similar to the ones we see in FIG. 3 (e)). In contrast to the net source-sink flow α_S^+ , the dispersal turnover α_C^+ may still be stabilizing for large values. Finally we find that no stability is possible for $\omega^{-+} < -0.5$ since $R_C^+ < R_C^-$.

Concerning the stability of larger metacommunities shown in figures 3 (b), (d), (f), and (h) we find that the stabilizing effects of large turnover rates still apply for the examined parameter sets, even though the overall stability is different. In the first case shown in 3 (b) we find that stability is actually larger for the metacommunity in the observed range of parameters. Intermediate regions of stability are found to be extended compared to the metapopulation.

VI. DISCUSSION AND CONCLUSION

In this paper, we have generalized the Master-Stability Function approach for meta-networks to systems with two types of patches. Combined with the Generalized Modelling approach, which allows to explore efficiently the linear stability of large networks, we have thus a powerful tool to evaluate the conditions under which large inhomogeneous meta-networks are stable. The advantages of the method come, however, at the cost of limiting the model to steady states that are identical on all patches of the same type and to biregular patch topologies. Nevertheless, previous work shows that results obtained with such restrictions are usually more generally valid [16].

We demonstrated the usefulness of the method by studying an explicit system, which is a meta-foodweb on a spatial network of sources and sinks. Often, the dynamics of source-sink systems are either modelled only with one patch of each type [4, 7, 39, 40] or with explicit population dynamics [4, 5, 7, 39–42] or both. The choice of population dynamics equations fixes the values of most exponent parameters, for instance logistic growth in sources implies $\phi^+ = 1$, $\mu^+ = 2$. Often the sinks are modelled with a positive local feedback such that they are unable to maintain a population without immigration. The exponent of dispersal is also fixed in these models. This means that no variation of the exponents is taken into account, and therefore the insights about the stability of steady states in these studies is very limited. The study by P. Amarasekare [7] varied the exponent s of emigration rates from the source and found that if $s > 1$ dispersal is stabilizing if large enough. The same was done for logistic growth in sinks with an identical result. In the light of our findings, these results are merely a special case: Logistic growth in sources corresponds to $\phi^+ = 1$, and s is the same exponent as our exponent ω^{-+} , such that the condition $\omega^{-+} > \phi^+$ is satisfied. The other exponents are chosen as $\hat{\omega}_i^{-+} = 0$ and $\mu^- = 1$ and fulfil our condition $\hat{\omega}_i^{-+} < \mu^-$.

Our approach thus allows a far broader investigation, not just for broad ranges of exponent parameters, but also for source-sink systems with more than two patches. Indeed, one source may be sustaining more than one sink and one sink can have more than one source as origin of its immigrating biomass [43]. Hence a biregular set of patches poses a generalization of the often used two-

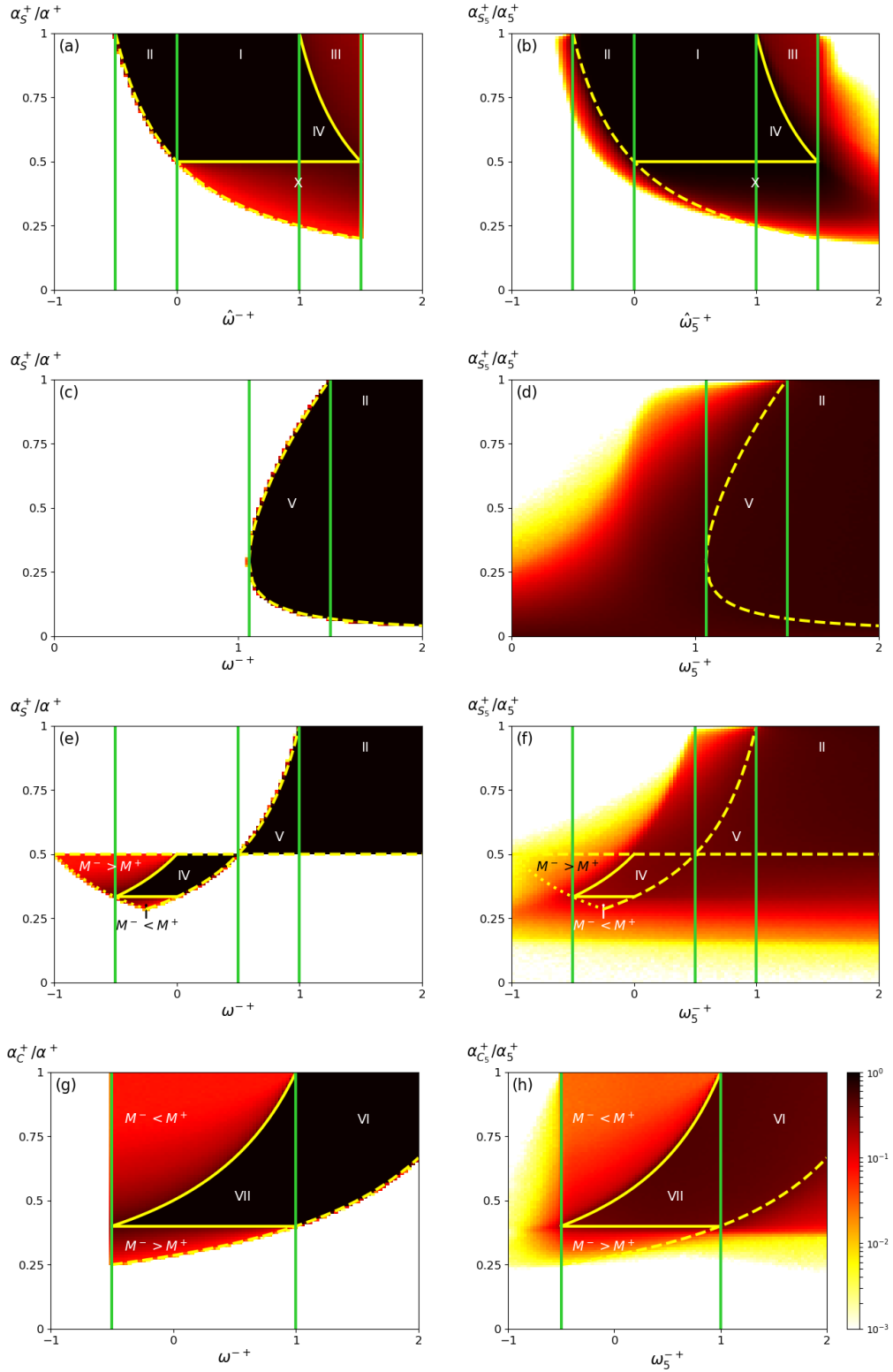


FIG. 3. The percentage of stable webs for metapopulations ((a), (c), (e), and (g)) or metacommunities with 10 species ((b), (d), (f), and (h)) in dependence of the source-sink flow $\alpha_{S_j}^+$ or dispersal turnover $\alpha_{C_i}^+$ and exponents of dispersal ω_i^{-+} or $\hat{\omega}_i^{-+}$. The model parameters used for each plot are shown in TABLE II. Several areas are marked with the corresponding stability criteria I-VII, which are bound by the roots (α_S^+ or α_C^+) of the determinant (33) (dashed yellow lines), the roots of the trace (32) (dotted yellow lines) or the roots of the additional eigenvalue λ_0 (23) (solid yellow lines). The vertical green lines indicate transitions when changing ω_i^{+-} or $\hat{\omega}_i^{+-}$. (Color online)

patch approximation. In fact, there are natural topologies which are close to bipartite sets of patches. In addition to the home ranges and roaming regions of higher animals mentioned in the Introduction, further examples are given by ponds in deserts or dry lands, mainland-island structures and landscapes sprinkled with lakes. Other examples with more than one patch of both types are mountains and valleys or lakes and rivers. More generally, each meta-foodweb where per-capita growth rates are distributed heterogeneously can be seen as a network of sources and sinks because some patches are net exporters of biomass, while others are net importers.

We found that two distinct types of dispersal related turnover rates emerge naturally from the generalized model framework. One is the dispersal turnover $\alpha_{C_i}^+$ which corresponds to the amount of biomass which is exchanged between sources and sinks. The other is the net source-sink flow α_S^+ which denotes the flow of biomass from sources to sinks and therefore the strength of source-sink dynamics. We performed an analytical evaluation of a metacommunity with only one species as well as a numerical evaluation of meta-foodwebs with many species in order to explore the capacity of both types of turnover rates to stabilize a system. In both situations, we found similar but not identical general conditions for such stabilizing effects. Stabilization can occur when rates become sufficiently large, but we also identified conditions under which a system is unstable for large and small rates but stable for an intermediate range of values of the rates. Such stabilizing effects of dispersal cannot occur in systems that are completely homogeneous [3].

We found two basic mechanisms which are stabilizing in source-sink dynamics for a single metapopulation, namely self regulation (i.e., a decrease of growth rate with population size), and negative feedback loops between source and sink populations. The net source-sink flow α_S^+ affects self regulation through local dynamics as well as through dispersal, and its increase stabilizes the system under suitable conditions. But even if an increased net source-sink flow reduces the ability of a population to self regulate, it can still have a stabilizing effect if it induces a negative feedback loop between source and sink populations. Conversely, a negative feedback loop between source and sink populations can destabilize dynamics even if the net source-sink flow increases self

regulation.

One particularly interesting finding is that dispersal can be stabilizing even if both patch types have a positive local feedback (36). This means that source-sink dynamics can stabilize metapopulations that are subject to strong local facilitation, which is equivalent to a positive local feedback. In particular, source-sink dynamics can be relevant for stabilizing not just sinks, but also sources. Sinks can provide mortality to source populations which would otherwise suffer from detrimental effects due to overcrowding. In contrast strong dispersal from sources to sinks may destabilize source populations (and thus possibly the whole source-sink system) due to the extent of losses [7]. Underestimating the importance of sinks coupled to these sources might have catastrophic consequences for ecosystems. Hence it is important to evaluate the interaction between sources and sinks. Since exponent parameters are relatively easy to obtain from data [44, 45] the findings of our study can be of practical use for identifying appropriate measures that preserve the stability of source-sink systems.

Another striking finding is that there exist generic conditions under which ecological and perceptual traps can be stable, even though dispersal is maladaptive in these situations. So far traps have mostly been seen as detrimental [46], but may provide a mechanism to stabilize metacommunities by limiting strong Allee-effects. Clearly further research is needed to identify the effects of traps on metacommunity persistence.

The listed general results are only a small part of what can still be achieved with the method. We expect that the formalism can be used to evaluate properties of other bipartite meta-networks, such as mutualistic ecological networks.

ACKNOWLEDGEMENTS

TG was supported by the Ministry for Science and Culture of Lower Saxony and the Volkswagen Foundation through the “Niedersächsisches Vorab” grant program (grant number ZN3285) This project was funded by the Deutsche Forschungsgemeinschaft (DFG, German Research Foundation) - grant number DR300/15.

-
- [1] A. M. Sauve, C. Fontaine, and E. Thébault, *Oikos* **123**, 378 (2014).
 - [2] T. Rohlf and S. Bornholdt, *Journal of theoretical biology* **261**, 176 (2009).
 - [3] A. Brechtel, P. Gramlich, D. Ritterskamp, B. Drossel, and T. Gross, *Physical Review E* **97**, 032307 (2018).
 - [4] R. D. Holt, *Theoretical population biology* **28**, 181 (1985).
 - [5] H. R. Pulliam, *The American Naturalist* **132**, 652 (1988).
 - [6] P. C. Dias, *Trends in Ecology & Evolution* **11**, 326 (1996).
 - [7] P. Amarasekare, *Journal of theoretical biology* **226**, 159 (2004).
 - [8] D. Gravel, N. Mouquet, M. Loreau, and F. Guichard, *The American Naturalist* **176**, 289 (2010).
 - [9] T. Gross and U. Feudel, *Physical Review E* **73**, 016205 (2006).
 - [10] L. M. Pecora and T. L. Carroll, *Physical Review Letters* **80**, 2109 (1998).
 - [11] H. Othmer and L. Scriven, *Journal of Theoretical Biology* **32**, 507 (1971).

- [12] L. A. Segel and S. A. Levin, in *AIP conference proceedings*, Vol. 27 (American Institute of Physics, 1976) pp. 123–152.
- [13] H. Nakao and A. S. Mikhailov, *Nature Physics* **6**, 544 (2010).
- [14] J. P. Gibert and J. D. Yeakel, *Theoretical Ecology* **12**, 265 (2019).
- [15] T. Gross, K. T. Allhoff, B. Blasius, U. Brose, B. Drossel, A. K. Fahimipour, C. Guill, J. D. Yeakel, and F. Zeng, *Philosophical Transactions of the Royal Society B: Biological Sciences* **375**, 20190455 (2020).
- [16] A. Brechtel, T. Gross, and B. Drossel, *Scientific reports* **9**, 1 (2019).
- [17] R. Ghorbanchian, J. G. Restrepo, J. J. Torres, and G. Bianconi, *Communications Physics* **4**, 120 (2021).
- [18] R. Mulas, C. Kuehn, and J. Jost, *Physical Review E* **101**, 062313 (2020).
- [19] J. E. Diffendorfer, *Oikos* , 417 (1998).
- [20] V. Remeš, *Oikos* **91**, 579 (2000).
- [21] M. Delibes, P. Gaona, and P. Ferreras, *The American Naturalist* **158**, 277 (2001).
- [22] B. A. Robertson and R. L. Hutto, *Ecology* **87**, 1075 (2006).
- [23] R. J. Fletcher Jr, J. L. Orrock, and B. A. Robertson, *Proceedings of the Royal Society B: Biological Sciences* **279**, 2546 (2012).
- [24] D. Szaz, G. Horvath, A. Barta, B. A. Robertson, A. Farkas, A. Egri, N. Tarjanyi, G. Racz, and G. Kriska, *PloS one* **10**, e0121194 (2015).
- [25] Á. Egri, Á. Pereszlényi, A. Farkas, G. Horváth, K. Penksza, and G. Kriska, *Journal of Insect Behavior* **30**, 374 (2017).
- [26] C. T. Lamb, G. Mowat, B. N. McLellan, S. E. Nielsen, and S. Boutin, *Journal of Animal Ecology* **86**, 55 (2017).
- [27] R. Hale, E. A. Trembl, and S. E. Swearer, *Proceedings of the Royal Society B: Biological Sciences* **282**, 20142930 (2015).
- [28] C. C. Paige and M. A. Saunders, *SIAM Journal on Numerical Analysis* **18**, 398 (1981).
- [29] G. Barabás, M. J. Michalska-Smith, and S. Allesina, *Nature ecology & evolution* **1**, 1870 (2017).
- [30] J. J. Gilroy and W. J. Sutherland, *Trends in ecology & evolution* **22**, 351 (2007).
- [31] M. A. Patten and J. F. Kelly, *Ecological Applications* **20**, 2148 (2010).
- [32] J. Battin, *Conservation Biology* **18**, 1482 (2004).
- [33] T. Gross, L. Rudolf, S. A. Levin, and U. Dieckmann, *Science* **325**, 747 (2009).
- [34] J. H. Brown and A. Kodric-Brown, *Ecology* **58**, 445 (1977).
- [35] A. Eriksson, F. Elías-Wolff, B. Mehlig, and A. Manica, *Proceedings of the royal society B: biological sciences* **281**, 20133127 (2014).
- [36] R. J. Williams and N. D. Martinez, *Nature* **404**, 180 (2000).
- [37] J. H. Brown, J. F. Gilgooly, A. P. Allen, V. M. Savage, and G. B. West, *Ecology* **85**, 1771 (2004).
- [38] S. B. Otto, B. C. Rall, and U. Brose, *Nature* **450**, 1226 (2007).
- [39] H. Wu, Y. Wang, Y. Li, and D. L. DeAngelis, *Theoretical Population Biology* **131**, 54 (2020).
- [40] H. Matsumoto and H. Seno, *Ecological modelling* **79**, 131 (1995).
- [41] R. Arditi, C. Lobry, and T. Sari, *Theoretical population biology* **106**, 45 (2015).
- [42] V. Bansaye and A. Lambert, *Theoretical population biology* **88**, 31 (2013).
- [43] R. Tittler, L. Fahrig, and M.-A. Villard, *Ecology* **87**, 3029 (2006).
- [44] D. A. FELL and H. M. SAURO, *European Journal of Biochemistry* **148**, 555 (1985).
- [45] J. D. Yeakel, D. Stiefs, M. Novak, and T. Gross, *Theoretical Ecology* **4**, 179 (2011).
- [46] R. Hale and S. E. Swearer, *Proceedings of the Royal Society B: Biological Sciences* **283**, 20152647 (2016).